Title

Chelating N-Heterocyclic Carbene Ligands Enable Tuning of Electrocatalytic CO_2 Reduction to Formate and Carbon Monoxide: Surface Organometallic Chemistry.

Journal

Angewandte Chemie (International ed. in English), 57(18)

ISSN

1433-7851

Authors

Cao, Zhi
Derrick, Jeffrey S
Xu, Jun
et al.

Publication Date

2018-04-01

DOI

10.1002/anie.201800367

Peer reviewed

Electrocatalysis

International Edition: DOI: 10.1002/anie.201800367
German Edition: DOI: 10.1002/ange.201800367

Chelating N-Heterocyclic Carbene Ligands Enable Tuning of Electrocatalytic CO_2 Reduction to Formate and Carbon Monoxide: Surface Organometallic Chemistry

Zhi Cao[+], Jeffrey S. Derrick[+], Jun Xu[+], Rui Gao, Ming Gong, Eva M. Nichols, Peter T. Smith, Xingwu Liu, Xiaodong Wen, Christophe Copéret, and Christopher J. Chang**

Abstract: *Reported here is the chelate effect as a design principle for tuning heterogeneous catalysts for electrochemical CO_2 reduction. Palladium functionalized with a chelating tris-N-heterocyclic carbene (NHC) ligand (Pd-timtmb^{Me}) exhibits a 32-fold increase in activity for electrochemical reduction of CO_2 to C1 products with high Faradaic efficiency ($FE_{C1} = 86\,\%$) compared to the parent unfunctionalized Pd foil ($FE = 23\,\%$), and with sustained activity relative to a monodentate NHC-ligated Pd electrode (Pd-mimtmb^{Me}). The results highlight the contributions of the chelate effect for tailoring and maintaining reactivity at molecular-materials interfaces enabled by surface organometallic chemistry.*

The chelate effect is a classic principle of molecular chemistry and it enables formation of metal-ligand coordination complexes with enhanced stability.[1] Given our interests in developing molecular approaches to hybrid catalyst platforms for electrochemical CO_2 reduction,[2] and drawing inspiration from the emerging use of N-heterocyclic carbenes (NHCs) as privileged ligands for influencing reactivity at metal surfaces,[3] we sought to explore the use of chelating NHC ligands to tune the reactivity of heterogeneous catalysts for electrochemical CO_2 reduction through surface organometallic chemistry. We now report that palladium electrodes functionalized with tridentate NHCs show enhanced activity and selectivity for electrochemical CO_2 reduction over parent unfunctionalized palladium counterparts, along with improved stability relative to palladium electrodes decorated with monodentate NHCs. By exploiting the chelate effect to achieve more robust attachment of molecular ligands to materials interfaces, this approach offers further opportunities to tailor heterogeneous catalysts and alter the surface with molecular-level precision.

Noting the catalytic organic transformations mediated by heterogeneous palladium, including asymmetric α-arylations,[3c] hydrogenations of olefins,[3j,m,u] and Buchwald–Hartwig aminations,[3w] as well as molecular Pd/NHC complexes used for reductive transformations of CO_2,[4] tripodal tris-NHCs were prepared by slightly modified literature methods[3t,5] to give the desired benchtop-stable tripodal tris-imidazolium bicarbonate salts ([timtmb^R(H)][$(HCO_3)_3$], R = Me, ^{i}Pr, ^{t}Bu; Scheme 1). Palladium-functionalized electrodes (Pd-timtmb^{Me}, Pd-timtmb^{iPr}, and Pd-timtmb^{tBu}) were then generated by soaking pretreated, thermally annealed palladium foils in 10 mM methanol solutions of [timtmb^R(H)]-[$(HCO_3)_3$] for 12 hours to generate the free tridentate carbenes, timtmb^R, in situ and washing with methanol to remove excess uncoordinated ligands. The resulting NHC-functionalized palladium electrodes were then dried, characterized, and evaluated for electrocatalytic studies.

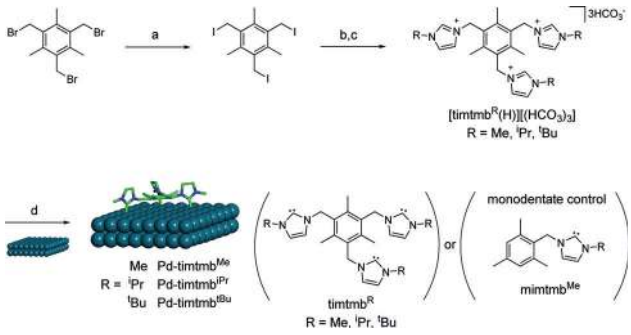

Scheme 1. Synthetic scheme for the preparation of tripodal N-heterocyclic carbenes and functionalization of palladium surfaces: a) NaI, Me_2CO, RT, 5 min; b) imidazole (1-methylimidazole, 1-isopropylimidazole, or 1-*tert*-butylimidazole), Me_2CO, RT, 5 h; c) CO_2, H_2O_2, RT, 1 h; d) MeOH, Pd foil.

[*] Dr. Z. Cao,[+] J. S. Derrick,[+] Dr. M. Gong, Dr. E. M. Nichols, P. T. Smith, Prof. C. J. Chang
Department of Chemistry, University of California
Berkeley, CA 94720 (USA)
E-mail: chrischang@berkeley.edu
Prof. C. J. Chang
Department of Molecular and Cell Biology, Howard Hughes Medical Institute, University of California
Berkeley, CA 94720 (USA)
J. S. Derrick,[+] Dr. M. Gong, Dr. E. M. Nichols, P. T. Smith, Prof. C. J. Chang
Chemical Sciences Division, Lawrence Berkeley National Laboratory
Berkeley, CA 94720 (USA)
Dr. J. Xu,[+] Prof. C. Copéret
Department of Chemistry and Applied Biosciences, ETH Zürich
Vladimir Prelog Weg 1–5, 8093 Zürich (Switzerland)
Dr. R. Gao, Dr. X. Liu, Prof. X. Wen
Institute of Coal Chemistry, Chinese Academy of Sciences
Taiyuan, Shanxi 030001 (China)
and
Synfuels China
Beijing, 100195 (China)
E-mail: wxd@sxicc.ac.cn
[+] These authors contributed equally to this work.
Supporting information and the ORCID identification number(s) for the author(s) of this article can be found under: https://doi.org/10.1002/anie.201800367.

The attachment of the timtmb^{Me} ligand to the palladium surface was first identified by high-resolution N1s X-ray photoelectron spectroscopy (XPS). The N1s peaks at 401.3 and 399.6 eV are consistent with previously reported spectra assigned to a surface-capped NHC layer,[3w] thus confirming the existence of timtmb^{Me} on the palladium surface (Pd-timtmb^{Me}; Figure 1 a). Additional analysis of the Pd-timtmb^{Me}

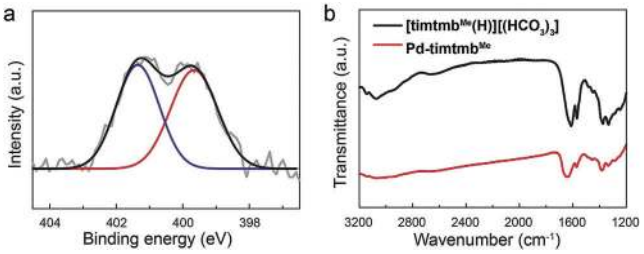

Figure 1. a) High-resolution XPS spectrum of N1s region of Pd-timtmb^{Me}. b) External-reflective IR spectra of [timtmb^{Me}(H)][(HCO$_3$)$_3$] and Pd-timtmb^{Me}.

electrode by external-reflection FT-IR spectroscopy shows two broad bands at about 1602 and 1339 cm^{-1}, which are consistent with C–C and C–N stretching vibrations of the imidazole[6] and are identical to those observed for [timtmb^{Me}-(H)][(HCO$_3$)$_3$], thus further supporting the successful functionalization of the electrode surface (Figure 1 b). Interaction of the tris-NHC ligands with the palladium surfaces was further reflected by the changes in ^{13}C NMR peaks resulting from interactions between the ^{13}C nuclei of the ligands and the Pd^0 surface,[2b,3w,6,7] which typically leads to broadening and shifting of resonance peaks as observed in the solid-state ^{13}C NMR spectra of [timtmb^{tBu}(H)][(HCO$_3$)$_3$] versus that of Pd-timtmb^{tBu} (see Figure S1 in the Supporting Information).

With characterization of the tripodal NHC-functionalized palladium surfaces in hand, we assessed the catalytic activity of the methyl-NHC derivative Pd-timtmb^{Me} for electrochemical CO_2 reduction, compared to that of the unmodified control palladium foil, in pH 7 aqueous media using 0.5 M $KHCO_3$ as the electrolyte. The current density was normalized to the geometric area of the working electrode and all potentials reported herein are referenced to the reversible hydrogen electrode (RHE). The Pd-timtmb^{Me} catalyst exhibits larger total current densities and positively shifted onset potentials relative to the control palladium foil according to cyclic voltammetry (CV) studies (Figure 2 a). The onset potential at −0.12 V, positively shifted by 265 mV relative to the palladium control, reflects a superior catalytic activity of NHC-functionalized Pd-timtmb^{Me} for electrochemical reduction of CO_2 in neutral aqueous media. No increase in current or anodic shift in onset potential was observed for NHC-functionalized palladium foils under Ar atmosphere, thus suggesting that this phenomenon is not the result of the reduction of surface-bound timtmb^{Me} (see Figure S2).

Controlled-potential electrolysis (CPE) experiments were performed in CO_2-saturated $KHCO_3$ buffer under different applied potentials between −0.37 V and −0.87 V to quantify the catalytic products of CO_2 reduction. Gaseous products were analyzed by gas chromatography (GC) and liquid products were characterized by ^{1}H NMR spectroscopy. Analysis of the head-space and electrolyte solutions following CPE experiments identified CO and H_2 as the gaseous products for both Pd-timtmb^{Me} and palladium foil as the catalyst while the functionalized electrode, Pd-timtmb^{Me}, generated a significant amount of formate relative to the unfunctionalized palladium electrode. The calculated Faradaic efficiencies (FEs) for C1

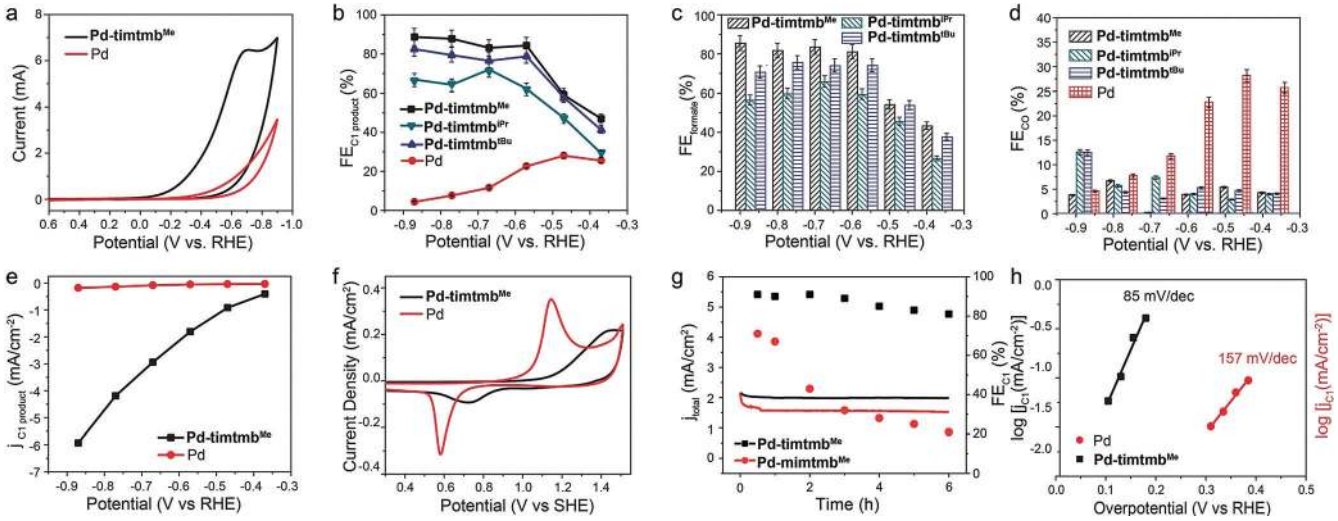

Figure 2. a) CV scans of Pd and Pd-timtmb^{Me} electrodes in CO_2-saturated 0.5 M $KHCO_3$ at pH 7.3. b) FEs of C1 product (CO for Pd; formate and CO for Pd-timtmb^R) produced by Pd and Pd-timtmb^R electrodes. c) FEs of formate generation by the Pd-timtmb^R electrodes. d) Faradaic efficiencies of CO generation by the Pd and Pd-timtmb^R electrodes. e) Specific current densities of C1 product generated by Pd and Pd-timtmb^{Me} electrodes. f) CO stripping voltammograms on Pd and Pd-timtmb^{Me} electrodes in 0.5 M H_2SO_4 electrolyte. The scan rate is 100 mV s^{-1}. g) CPE of tridentate-NHC Pd-mimtmb^{Me} and monodentate-NHC Pd-timtmb^{Me} electrodes at −0.57 V over a 6 h time course. h) Tafel plots of Pd and Pd-timtmb^{Me} electrodes.

products (formate and CO) for Pd-timtmb^{R} and unmodified palladium are shown in Figure 2b. The Pd-timtmb^{R} catalysts show higher FEs for C1 products compared to the control palladium foil at all potentials examined. At a potential of −0.57 V, the Pd-timtmb^{Me} catalyst displays an optimal FE for C1 production (FE = 86%; 82% of formate and 4% of CO) with a moderate overpotential of 360 mV (Figures 2c and d), with the remaining current going to H_2 production. The control palladium foil shows a peak FE of 23% with CO as the major C1 product. For comparison, the FEs of both Pd-timtmb^{iPr} and Pd-timtmb^{tBu} were obtained and also show improved formate selectivity (Figure 2c) over the control palladium, but slightly lower than Pd-timtmb^{Me}. In addition to the superior selectivity of Pd-timtmb^{Me} for CO_2 reduction products, Pd-timtmb^{Me} also showed significantly enhanced specific current densities (j_{C1}) at all potential ranges compared to the unfunctionalized palladium foil. Indeed, at the applied potential of −0.57 V, Pd-timtmb^{Me} exhibits a 32-fold increase in specific current density compared to the unfunctionalized palladium foil (Figure 2e).

To evaluate the contributions of the timtmb^{Me} ligand to the observed improvements in catalytic activity and selectivity, we first investigated the electrochemically active surface area (ECSA) of the palladium foil with and without timtmb^{Me} functionalization by a CO stripping method (Figure 2f).[8] The calculated ECSA of Pd-timtmb^{Me} is 51% of the unmodified palladium foil, presumably resulting from the occupation of palladium sites by timtmb^{Me} ligands on the surface. Despite its smaller ECSA relative to control palladium foil, the higher activity and selectivity for CO_2 reduction observed on Pd-timtmb^{Me} shows the high intrinsic activity of the molecular-materials interface formed by NHC ligation. Another interesting factor extracted from the CO stripping voltammograms is the observed positive shift of the anodic CO oxidation peak upon timtmb^{Me} functionalization, which is suggestive of increased electron density on palladium surface by NHC functionalization and may contribute to the activity for electrochemical CO_2 reduction.

Longer-term CPE experiments at a potential of −0.57 V vs. RHE show that the Pd-timtmb^{Me} catalyst maintains activity and high FE for C1 product-formation for up to 6 hours (Figure 2g). To evaluate the contributions of the chelate effect to catalyst stability, we prepared a monodentate NHC analogue (mimtmb^{Me}; see Scheme S1) and made a functionalized palladium foil in MeOH to generate Pd-mimtmb^{Me}. First, to explore possible differences in coordination modes between the tridentate timtmb^{Me} and the monodentate mimtmb^{Me} ligands with the palladium surface, differences resulting from the decreased steric bulk associated with the elimination of two of the NHC arms, CO stripping voltammograms were measured for Pd-mimtmb^{Me}.[9] As can be seen in Figure S3, the CO stripping voltammogram for Pd-mimtmb^{Me} was similar to that of Pd-timtmb^{Me} but with a slightly smaller CO oxidation peak. The positive shift in the CO stripping peak suggests that a similar σ-donation effect exists between mimtmb^{Me} and the palladium surface. Taken together, these results suggest a similar interaction mode between mimtimb^{Me} and timtmb^{Me} with the palladium electrode, with mimtmb^{Me} having a slightly higher surface coverage than Pd-timtmb^{Me}. To further deconvolute the role of coordination modes from denticity in this system, a more thorough molecular level investigation into the exact coordination chemistry of these molecules to metallic surfaces will be the subject of future study. CPE experiments under CO_2 atmosphere with Pd-mimtmb^{Me} show that Pd-mimtmb^{Me} does enhance the electrocatalysis of CO_2 compared to native palladium foil at early time points, however it exhibits inferior stability and activity over the same 6 hour time period as reflected by the significant FE loss for C1 down to less than 40% within 2 hours of electrolysis (Figure 2g). These data suggest that the chelate effect may be essential for maintaining electrochemical activity for selective CO_2 reduction.

The stability of Pd-timtmb^{Me} under electrochemical conditions was further evaluated by FT-IR, double-layer capacitance,[10] and XPS measurements. Indeed, the Pd-timtmb^{Me} catalyst possesses nearly identical FT-IR features prior to and immediately after electrolysis, thus reflecting its electrochemical durability (see Figure S4). Furthermore, the electrochemically accessible palladium surface area for the same Pd-timtmb^{Me} working electrode before and after electrolysis is nearly identical as evidenced by only subtle observed differences in measured area for double-layer capacitance (see Figures S4 and S5). Moreover, high-resolution N1s XPS peaks are persistent after bulk electrolysis, thus confirming the existence of timtmb^{Me} on the palladium surface (see Figure S6) throughout the reaction.

We next explored the kinetics of CO_2 reduction on the control palladium and NHC-functionalized palladium electrodes using Tafel analysis (Figure 2h). The data establish that NHC functionalization influences the mechanistic pathways for CO_2 reduction. A Tafel slope of 157 mV/decade is observed for the control palladium, and is comparable to the 118 mV/decade expected for rate-limiting single-electron transfer from the adsorbed CO_2 to generate the surface adsorbed $CO_2^{\bullet-}$.[11] In contrast, the Tafel slope for Pd-timtmb^{Me} is 85 mV/decade, thus reflecting the possibility that Pd-timtmb^{Me} may undergo a pre-equilibrating one-electron transfer followed by a rate-limiting chemical step. Strong σ-donation from the NHC ligands can make the palladium surface of Pd-timtmb^{Me} more electron-rich, which in turn can promote fast electron transfer to CO_2 prior to the rate-determining step.

Finally, we performed DFT calculations to further probe the effects of NHC ligation on the palladium surface and its reactivity consequences. In particular, we computed the possible pathways of CO_2 hydrogenation into HCOOH on two surface models of Pd(111) and Pd(111)-timtmb^{Me} (Figure 3 and Figure S7). The initial step of CO_2 hydrogenation ($CO_2 + H^* \rightarrow COOH^*$) generates COOH*, a key reaction intermediate of CO_2 reduction,[3d,f,i,q–s,v,12] with an energy barrier of 0.85 eV for Pd-timtmb^{Me}, compared to a 1.23 eV barrier for a parent Pd(111) surface, thus reflecting a more energetically favored pathway for COOH* formation on Pd-timtmb^{Me}. HCOOH formation was further computed by COOH* hydrogenation on the two models. For $COOH^* + H^* \rightarrow HCOOH$, the calculated barriers are 1.24 and 1.00 eV on Pd(111) and Pd(111)-timtmb^{Me}, thus indicating that HCOOH formation on Pd-timtmb^{Me} over the control palla-

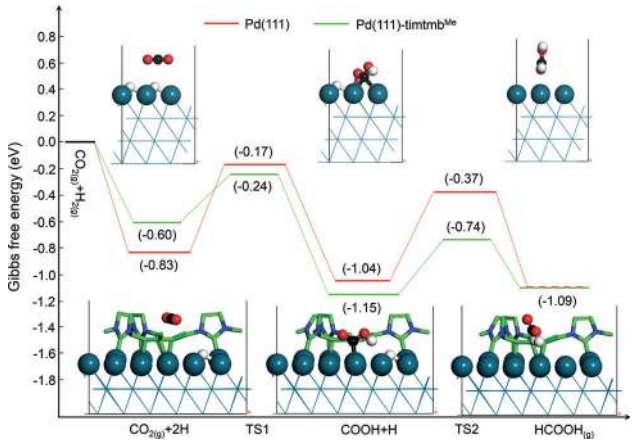

Figure 3. Free-energy diagrams for CO_2 reduction to HCOOH on Pd(111) and Pd(111)-timtmb^{Me}.

dium is favored as well. These computational findings are consistent with the experimental observations that formate is formed as the dominant C1 product in Pd-timtmb^{Me}-mediated CO_2 reduction. CO formation on the Pd(111)-timtmb^{Me} is predicted to be energetically unfavored as reflected by the larger required energy compared with Pd(111) (see Figure S8). Moreover, the improved electrochemical stability of Pd-NHC electrodes, formed from tridentate versus monodentate NHCs effect arising from timtmb^{Me} functionalization, is calculated to be borne out by the significantly favored adsorption energy of Pd(111)-timtmb^{Me} (−1.21 eV) relative to Pd(111) (−0.39 eV), as shown by our DFT calculations (see Figure S9).

Taken together, this work establishes the chelate effect as a molecular design approach for tuning heterogeneous catalysts, as illustrated by observed improvements in activity, selectivity, and stability for electrochemical CO_2 reduction on palladium electrodes modified through tris-NHC ligation. We anticipate that this surface organometallic chemistry strategy,[13] in which molecular-material analogues to homogeneous coordination complexes can be developed and studied, will be applicable for a broader range of catalytic processes and other applications.

Acknowledgements

Financial support for catalysis, including synthesis, and electrochemical measurements, was provided by U.S. Department of Energy/Lawrence Berkeley National Laboratory Grant 101528-002 (C.J.C.). C.J.C. is an Investigator with the Howard Hughes Medical Institute and a CIFAR Senior Fellow. E.M.N. and P.T.S. thank the National Science Foundation for Graduate Fellowships. X.D.W. is grateful for the financial support from the National Natural Science Foundation of China (No. 21473229 and No. 91545121). X.D.W. also acknowledges Hundred-Talent Program of Chinese Academy of Sciences, Shanxi Hundred-Talent Program and National Thousand Young Talents Program of China.

Conflict of interest

The authors declare no conflict of interest.

Keywords: CO_2 reduction · electrocatalysis · N-heterocyclic carbenes · palladium · surface chemistry

How to cite: *Angew. Chem. Int. Ed.* **2018**, *57*, 4981–4985
Angew. Chem. **2018**, *130*, 5075–5079

[1] A. F. Cotton, G. Wilkinson, M. Bochmann, C. A. Murillo, M. Bochmann, *Advanced Inorganic Chemistry*, 6th ed., Wiley, New York, **1999**.

[2] a) S. Lin, C. S. Diercks, Y.-B. Zhang, N. Kornienko, E. M. Nichols, Y. Zhao, A. R. Paris, D. Kim, P. Yang, O. M. Yaghi, C. J. Chang, *Science* **2015**, *349*, 1208–1213; b) Z. Cao, D. Kim, D. Hong, Y. Yu, J. Xu, S. Lin, X. Wen, E. M. Nichols, K. Jeong, J. A. Reimer, P. Yang, C. J. Chang, *J. Am. Chem. Soc.* **2016**, *138*, 8120–8125; c) M. Gong, Z. Cao, W. Liu, E. M. Nichols, P. T. Smith, J. S. Derrick, Y.-S. Liu, J. Liu, X. Wen, C. J. Chang, *ACS Cent. Sci.* **2017**, *3*, 1032–1040.

[3] a) E. C. Hurst, K. Wilson, I. J. Fairlamb, V. Chechik, *New J. Chem.* **2009**, *33*, 1837–1840; b) J. Vignolle, T. D. Tilley, *Chem. Commun.* **2009**, 7230–7232; c) K. V. Ranganath, J. Kloesges, A. H. Schäfer, F. Glorius, *Angew. Chem. Int. Ed.* **2010**, *49*, 7786–7789; *Angew. Chem.* **2010**, *122*, 7952–7956; d) P. Lara, O. Rivada-Wheelaghan, S. Conejero, R. Poteau, K. Philippot, B. Chaudret, *Angew. Chem. Int. Ed.* **2011**, *50*, 12080–12084; *Angew. Chem.* **2011**, *123*, 12286–12290; e) A. V. Zhukhovitskiy, M. G. Mavros, T. Van Voorhis, J. A. Johnson, *J. Am. Chem. Soc.* **2013**, *135*, 7418–7421; f) D. Gonzalez-Galvez, P. Lara, O. Rivada-Wheelaghan, S. Conejero, B. Chaudret, K. Philippot, P. W. van Leeuwen, *Catal. Sci. Technol.* **2013**, *3*, 99–105; g) C. M. Crudden, J. H. Horton, I. I. Ebralidze, O. V. Zenkina, A. B. McLean, B. Drevniok, Z. She, H.-B. Kraatz, N. J. Mosey, T. Seki, *Nat. Chem.* **2014**, *6*, 409–414; h) E. A. Baquero, S. Tricard, J. C. Flores, E. de Jesús, B. Chaudret, *Angew. Chem. Int. Ed.* **2014**, *53*, 13220–13224; *Angew. Chem.* **2014**, *126*, 13436–13440; i) P. Lara, A. Suárez, V. Collière, K. Philippot, B. Chaudret, *ChemCatChem* **2014**, *6*, 87–90; j) C. Richter, K. Schaepe, F. Glorius, B. J. Ravoo, *Chem. Commun.* **2014**, *50*, 3204–3207; k) A. V. Zhukhovitskiy, M. J. MacLeod, J. A. Johnson, *Chem. Rev.* **2015**, *115*, 11503–11532; l) M. J. MacLeod, J. A. Johnson, *J. Am. Chem. Soc.* **2015**, *137*, 7974–7977; m) A. L. Ferry, K. Schaepe, P. Tegeder, C. Richter, K. M. Chepiga, B. J. Ravoo, F. Glorius, *ACS Catal.* **2015**, *5*, 5414–5420; n) L. M. Martínez-Prieto, A. Ferry, P. Lara, C. Richter, K. Philippot, F. Glorius, B. Chaudret, *Chem. Eur. J.* **2015**, *21*, 17495–17502; o) G. Wang, A. Rühling, S. Amirjalayer, M. Knor, J. B. Ernst, C. Richter, H.-J. Gao, A. Timmer, H.-Y. Gao, N. L. Doltsinis, F. Glorius, H. Fuchs, *Nat. Chem.* **2017**, *9*, 152–156; p) P. Lara, L. Martínez-Prieto, M. Roselló-Merino, C. Richter, F. Glorius, S. Conejero, K. Philippot, B. Chaudret, *Nano-Struct. Nano-Objects* **2016**, *6*, 39–45; q) J. B. Ernst, S. Muratsugu, F. Wang, M. Tada, F. Glorius, *J. Am. Chem. Soc.* **2016**, *138*, 10718–10721; r) L. Martínez-Prieto, A. Ferry, L. Rakers, C. Richter, P. Lecante, K. Philippot, B. Chaudret, F. Glorius, *Chem. Commun.* **2016**, *52*, 4768–4771; s) A. Fedorov, H.-J. Liu, H.-K. Lo, C. Copéret, *J. Am. Chem. Soc.* **2016**, *138*, 16502–16507; t) C. M. Crudden, J. H. Horton, M. R. Narouz, Z. Li, C. A. Smith, K. Munro, C. J. Baddeley, C. R. Larrea, B. Drevniok, B. Thanabalasingam, *Nat. Commun.* **2016**, *7*, 12654; u) A. Rühling, K. Schaepe, L. Rakers, B. Vonhören, P. Tegeder, B. J. Ravoo, F. Glorius, *Angew. Chem. Int. Ed.* **2016**, *55*, 5856–5860; *Angew. Chem.* **2016**, *128*, 5950–5955; v) L. M. Martínez-Prieto, L. Rakers, A. M. López-Vinasco, I. Cano, Y. Coppel, K. Philippot, F. Glorius, B. Chaudret, P. W. van Leeuwen, *Chem.*

Eur. J. **2017**, *23*, 12779 – 12786; w) J. B. Ernst, C. Schwermann, G.-i. Yokota, M. Tada, S. Muratsugu, N. L. Doltsinis, F. Glorius, *J. Am. Chem. Soc.* **2017**, *139*, 9144 – 9147; x) K. Salorinne, R. W. Man, C. H. Li, M. Taki, M. Nambo, C. M. Crudden, *Angew. Chem. Int. Ed.* **2017**, *56*, 6198 – 6202; *Angew. Chem.* **2017**, *129*, 6294 – 6298.

[4] a) J. A. Therrien, M. O. Wolf, B. O. Patrick, *Inorg. Chem.* **2014**, *53*, 12962 – 12972; b) J. A. Therrien, M. O. Wolf, B. O. Patrick, *Inorg. Chem.* **2015**, *54*, 11721 – 11732; c) J. A. Therrien, M. O. Wolf, *Inorg. Chem.* **2017**, *56*, 1161 – 1172.

[5] a) H. Nakai, Y. Tang, P. Gantzel, K. Meyer, *Chem. Commun.* **2003**, 24 – 25; b) H. R. Dias, W. Jin, *Tetrahedron Lett.* **1994**, *35*, 1365 – 1366.

[6] T. Fahlbusch, M. Frank, J. Schatz, H. Schmaderer, *Eur. J. Org. Chem.* **2006**, 1899 – 1903.

[7] M. Planellas, R. Pleixats, A. Shafir, *Adv. Synth. Catal.* **2012**, *354*, 651 – 662.

[8] a) A. Klinkova, P. D. Luna, C.-T. Dinh, O. Voznyy, E. M. Larin, E. Kumacheva, E. H. Sargent, *ACS Catal.* **2016**, *6*, 8115 – 8120; b) A. S. Bauskar, C. A. Rice, *Electrochim. Acta* **2013**, *93*, 152 – 157.

[9] a) R. W. Y. Man, C.-H. Li, M. W. A. MacLean, O. V. Zenkina, M. T. Zamora, L. N. Saunders, A. Rousina-Webb, M. Nambo, C. M. Crudden, *J. Am. Chem. Soc.* **2018**, *140*, 1576 – 1579; b) L. Jiang, B. Zhang, G. Medard, A. P. Seitsonen, F. Haag, F. Allegretti, J. Reichert, B. Kuster, J. V. Barth, A. C. Papageorgiou, *Chem. Sci.* **2017**, *8*, 8301 – 8308; c) C. R. Larrea, C. J. Baddeley, M. R. Narouz, N. J. Mosey, J. H. Horton, C. M. Crudden, *ChemPhysChem* **2017**, *18*, 3536 – 3539.

[10] a) P. Waszczuk, P. Zelenay, J. Sobkowski, *Electrochim. Acta* **1995**, *40*, 1717 – 1721; b) C. W. Li, J. Ciston, M. W. Kanan, *Nature* **2014**, *508*, 504 – 507.

[11] Y. Chen, M. W. Kanan, *J. Am. Chem. Soc.* **2012**, *134*, 1986 – 1989.

[12] J. T. Feaster, C. Shi, E. R. Cave, T. Hatsukade, D. N. Abram, K. P. Kuhl, C. Hahn, J. K. Nørskov, T. F. Jaramillo, *ACS Catal.* **2017**, *7*, 4822 – 4827.

[13] C. Copéret, A. Comas-Vives, M. P. Conley, D. P. Estes, A. Fedorov, V. Mougel, H. Nagae, F. Nunez-Zarur, P. A. Zhizhko, *Chem. Rev.* **2016**, *116*, 323 – 421.

Manuscript received: January 10, 2018
Revised manuscript received: February 27, 2018
Accepted manuscript online: March 1, 2018
Version of record online: March 22, 2018

